Long-Term Stability of Satellites in Non-Equatorial Orbits

Vignesh Karthikeyan

Abstract: In the present day, around 9900 satellites are orbiting the Earth. To further understand and model these orbits, this paper introduces a dynamics model aimed at achieving higher fidelity in orbit simulations, accounting for different angles, velocities, positions, and accelerations. Additionally, perturbations in space and their effects on various types of orbits are studied. Three major perturbations are tested: third-body perturbations, Earth's oblateness (J2 effect), and atmospheric drag. After plotting these orbits, it was discovered that the most significant perturbation to Earth-orbiting objects is the J2 effect, followed by atmospheric drag and third-body perturbations. While these perturbations may seem to have a minuscule effect on orbits, the numbers, especially those resulting from the J2 effect, can be incredibly significant in orbital mechanics, where calculations must be precise. The insights gained from this project highlight the necessity of using advanced models and real-time data to refine predictions and ensure satellites' precise and stable operation. By continuously improving the understanding and modeling of these perturbations, the reliability and effectiveness of satellite missions are enhanced, which are integral to space exploration, communication, navigation, and Earth observation.

Introduction

Space exploration is driven by humanity’s insatiable curiosity and thirst for knowledge, offering both intrinsic and extrinsic benefits that make it a necessity in today’s world. At its core, space exploration seeks to unravel the mysteries of the universe, deepening the understanding of the cosmos and advancing fields such as astrophysics and cosmology. By utilizing cutting-edge instruments like probes, satellites, and telescopes, scientists gather invaluable data about celestial bodies and the universe’s natural state, contributing to groundbreaking discoveries about black holes, dark matter, and the origins of life. The search for other potential habitats and intelligent life on exoplanets is a crucial aspect of space exploration, providing insights into whether we are alone in the universe and the conditions necessary to support life beyond Earth. The technological challenges of space exploration drive innovation, leading to advancements with far-reaching applications on Earth, from cell phone cameras and solar panels to the indispensable Global Positioning System (GPS). The economic benefits of space exploration are substantial, fostering job creation and economic growth through the collaborative efforts of government space agencies and private companies. Furthermore, space exploration

enhances the ability to detect and mitigate near-Earth objects (NEOs) that could threaten the planet, providing critical tools and knowledge for planetary defense. As Earth's resources become strained, space colonization emerges as a potential solution for humanity's long-term survival, with efforts to establish a presence on Mars or other celestial bodies offering valuable lessons in sustainable living. Space exploration also fosters international cooperation and diplomacy, as evidenced by the collaborative nature of the International Space Station (ISS), which unites space agencies from multiple countries in a shared mission. This collaborative spirit promotes peaceful interaction, trust, and the exchange of expertise among nations. The endeavor of space exploration inspires society by showcasing human creativity, critical thinking, and problem-solving skills, essential for addressing global challenges. It cultivates a culture that values education, innovation, and the relentless pursuit of knowledge, inspiring future generations to pursue careers in science, technology, engineering, and mathematics (STEM). The transformative nature of space exploration, with its capacity to improve humanity and foster a sense of interconnectedness, makes it a journey of self-discovery and a testament to the unwavering human spirit. As other planets are explored and the universe's mysteries are contemplated, space exploration remains a vital and inspiring pursuit that advances our understanding and betterment of life on Earth.

Humans have always gazed at the night sky with wonder, dreaming of the vast expanse of space. By the mid-20th century, these dreams began to transform into reality with the advent of rockets capable of achieving orbital velocities. The foundation for space exploration was laid with the development of long-distance rockets by Nazi Germany in the 1930s and 1940s, notably the V-2 missiles used during World War II. Following the war, the United States and the Soviet Union accelerated their missile programs, leading to groundbreaking achievements. The launch of the Soviet Union's Sputnik 1 in 1957 marked the first artificial satellite to orbit Earth, igniting the space race. Yuri Gagarin's historic orbit in 1961 made him the first human in space, followed by the United States launch of Explorer 1 in 1958 and John Glenn's orbit in 1962. The pinnacle of early space exploration was the Apollo program, with President Kennedy's goal of landing a man on the Moon realized on July 20, 1969, when Neil Armstrong took his "giant leap for mankind." Between 1969 and 1972, six Apollo missions further explored the Moon, providing invaluable scientific data. Unmanned spacecraft like the Mariner and Voyager missions significantly contributed by photographing and probing the Moon, Mars, and other celestial bodies. The 1970s saw the launch of Skylab, America's first space station, and the Apollo-Soyuz Test Project, the first international crewed space mission. The 1980s were marked by the Space Shuttle program, which revolutionized space missions by enabling satellite deployment, scientific research, and the construction of the International Space Station (ISS), despite tragic setbacks with the Challenger and Columbia disasters. The Gulf War highlighted the strategic importance of space-based assets, with satellites providing critical intelligence. The ISS, continuously occupied since 2000, symbolizes international cooperation, hosting astronauts and researchers from around the world. Advances in space launch systems have aimed to reduce costs and improve reliability, with various nations and private companies competing in the commercial launch market. Today, modern space exploration pushes the boundaries of what is possible, focusing on Mars with NASA and its partners sending orbiters, landers, and rovers to gather data and prepare for human missions. The Curiosity Rover's radiation data and the MARS 2020 Rover's exploration of Martian resources are paving the way for manned missions to the Red Planet, targeted for the 2030s, reflecting humanity's relentless pursuit of knowledge

and spirit of discovery. Orbital mechanics, in particular, has played a crucial role in the success of human space missions, from the precise calculation of launch windows for Apollo missions to the navigation of rovers on Mars. This field has enabled the planning and execution of complex trajectories and maneuvers, ensuring that spacecraft reach their intended destinations and perform their missions effectively.

Orbital mechanics, or astrodynamics, is defined as the application of celestial mechanics and ballistics to practical problems involving the motion of spacecraft, such as rockets and satellites. By employing Newton's laws of motion and universal gravitation, this field is central to determining spacecraft trajectories, executing orbital maneuvers, and planning interplanetary transfers, all crucial for successful space missions. It primarily focuses on the dynamics of artificial objects in space, although it is rooted in the broader study of celestial mechanics, which encompasses the motion of natural astronomical bodies like planets, moons, and comets. According to the NASA Earth Observatory, the evolution of orbital mechanics traces back to Johannes Kepler’s early 17th-century work on planetary orbits and Isaac Newton’s formulation of the laws of motion and universal gravitation. Advances continued with contributions from Leonhard Euler and Carl Friedrich Gauss, who refined methods for orbit determination. The field saw significant development in the 20th century with Samuel Herrick’s pioneering work and the integration of numerical techniques and powerful computers, which enabled precise space navigation and mission planning. Today, orbital mechanics remains a vital discipline, essential for operating and navigating satellites and space probes, and continues to leverage both classical mechanics and, when necessary, the more accurate predictions provided by general relativity for complex, high-gravity scenarios.

Perturbations in orbital mechanics encompass the various external forces and effects that cause deviations from the idealized orbits predicted by Kepler's laws. These perturbations significantly impact the long-term stability of satellites, particularly those in non-equatorial orbits. Gravitational perturbations from celestial bodies such as the Moon and the Sun introduce additional forces that can alter a satellite's trajectory over time, leading to deviations that require frequent adjustments to maintain mission objectives. For satellites in low Earth orbit (LEO), atmospheric drag plays a prominent role; despite the thinness of Earth's atmosphere at these altitudes, residual atmospheric particles create a frictional force that gradually slows the satellite's orbital speed, leading to a continuous decrease in altitude and eventual orbital decay if corrective measures are not applied. Earth's oblateness, due to its equatorial bulge, causes variations in the gravitational field experienced by the satellite, which introduces complexities such as precession and nodal regression that can affect the satellite's orbital parameters and contribute to long-term changes. Understanding and modeling these perturbations are crucial not only for predicting satellite behavior but also for ensuring the accuracy and stability of satellite operations. Their significance lies in their impact on mission planning, satellite longevity, and the ability to execute long-term objectives in space.

To further understand and model orbits, this paper introduces a dynamics model aimed at achieving higher fidelity in orbit simulations, accounting for different angles, velocities, positions, and accelerations. Additionally, perturbations in space and their effects on various types of orbits are examined. Three major perturbations are considered: third-body perturbations, Earth's oblateness (J2 effect), and atmospheric drag. By analyzing the orbital variations, it is determined

that the most significant perturbation to Earth-orbiting objects is the J2 effect, followed by atmospheric drag and third-body perturbations. While the effects of these perturbations may seem minuscule, their impact, especially from the J2 effect, can be incredibly significant in orbital mechanics, where precision is paramount. The insights gained from this project underscore the necessity of using advanced models and real-time data to refine predictions and ensure satellites' precise and stable operation. Continuously improving the understanding and modeling of these perturbations enhances the reliability and effectiveness of satellite missions, which are integral to space exploration, communication, navigation, and Earth observation.

Orbital Mechanics

Keplerian Motion

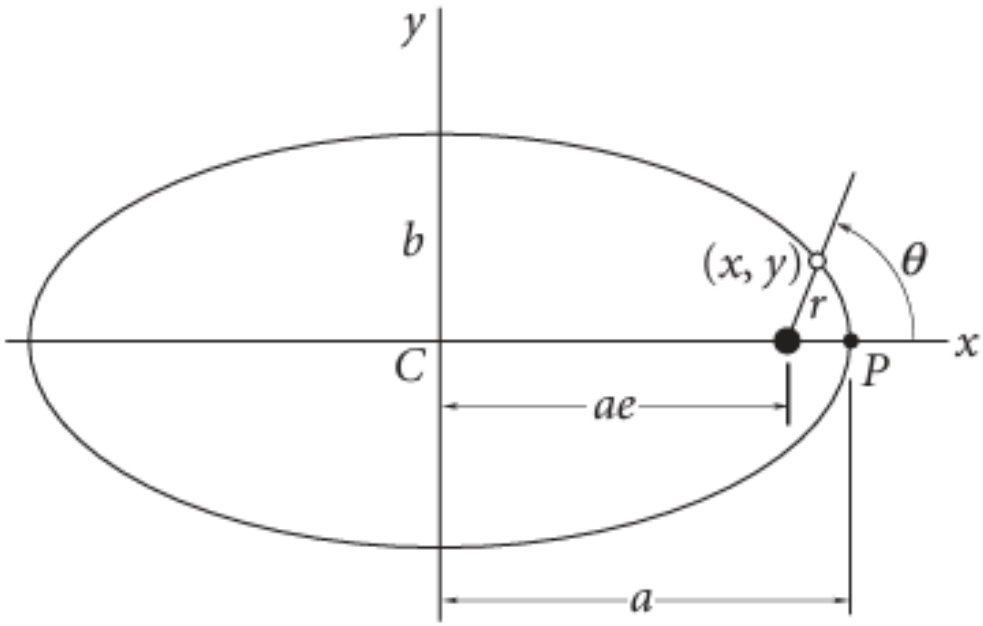

Graph from *Space Traffic Management* by Carolin Frueh
Figure 1: Illustration of the Orbital Elements in WCS

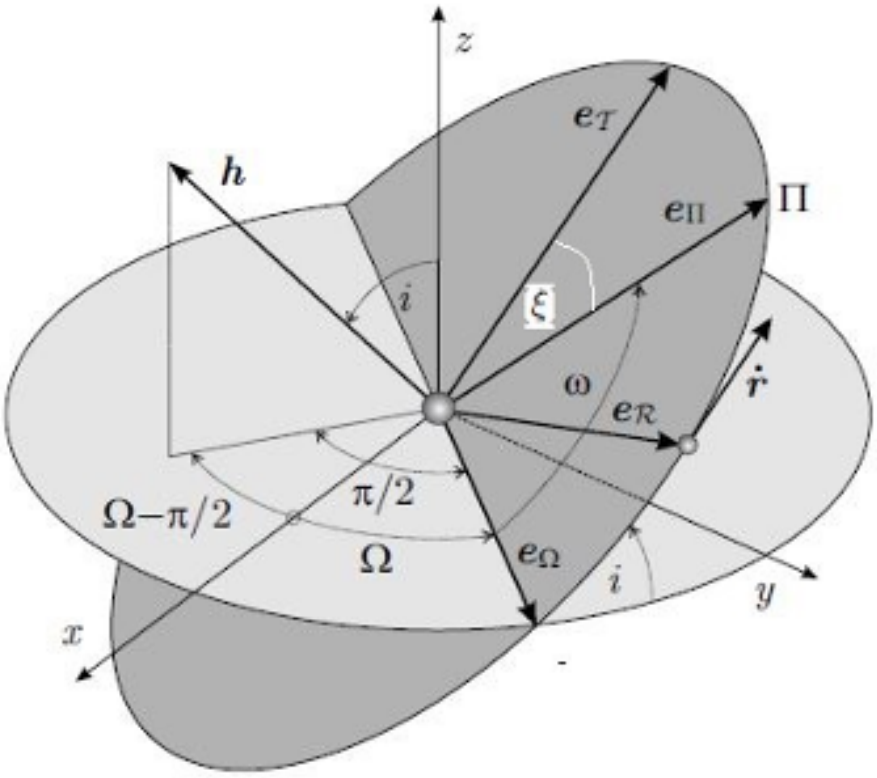

Graph from *Space Traffic Management* by Carolin Frueh

Figure 2: Illustration of the orbital elements in the ECI coordinate system

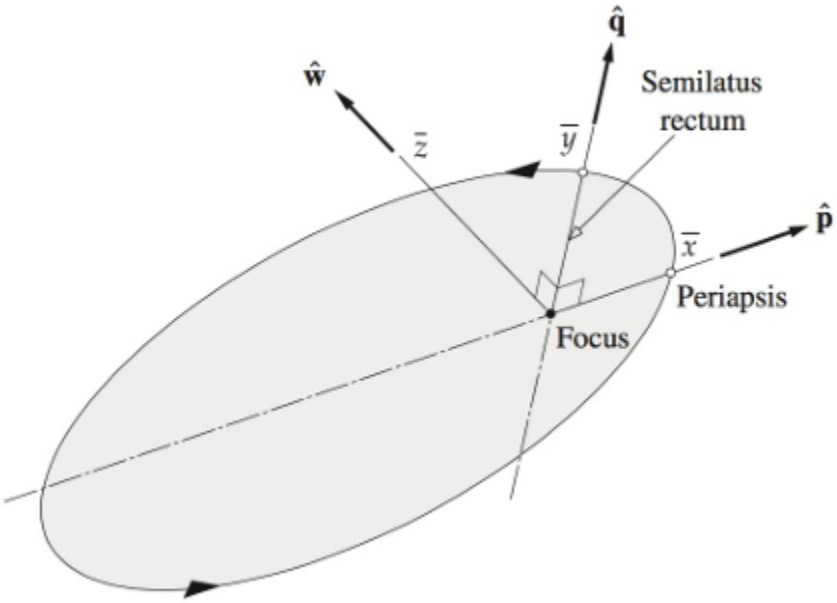

Graph from *Space Traffic Management* by Carolin Frueh
Figure 3: Illustration of the orbital elements in the Cartesian coordinate system

Two-body motion in orbital mechanics, specifically Keplerian motion, involves the gravitational interaction between two bodies where one body orbits the other. This interaction can result in four different types of trajectories: circular, elliptical, parabolic, and hyperbolic. However, this discussion focuses on elliptical orbits, as described by Kepler's laws. When analyzing satellite motion, it is typically assumed that the smaller body (the satellite) does not perturb the larger body (Earth) due to its significantly smaller mass. According to Kepler's first law, the orbit of the satellite is an ellipse with the Earth at one focus. The second law, the law of equal areas, states that a line segment joining the satellite and Earth sweeps out equal areas during equal time intervals, leading to variable orbital speed depending on the satellite's position in its orbit. The third law establishes a relationship between the orbital period and the semi-major axis, stating that the square of the orbital period is proportional to the cube of the semi-major axis. Key parameters, known as Keplerian elements, define the orbit's size (semi-major axis(**a**)), shape (eccentricity(**e**)), orientation (inclination(**i**), longitude of ascending node(**Ω**), and argument of periapsis(**ω**)), and position of the orbiting body at a given time (true anomaly). These elements enable precise predictions of orbital paths, essential for satellite operations and space mission planning.

Key 2 body Equations:

In orbital mechanics, understanding the dynamics of celestial bodies requires a set of key equations that describe their interactions and motions within a two-body system. These equations provide insights into the total energy, relative velocity, and orbital characteristics of the bodies involved.

The total energy equation is given by:

$$E_{tot} = \frac{1}{2}m_1\frac{\delta\bar{x_1}}{\delta t} + \frac{1}{2}m_2\frac{\delta\bar{x_2}}{\delta t} + U(r) = \frac{1}{2}(m_1 + m_2)\frac{\delta\bar{R}}{\delta t}^2 + \frac{1}{2}\mu\frac{\delta\bar{r}}{\delta t}^2 + U(r) \quad (1)$$

Equation 1 represents the total energy in a two-body system, combining kinetic and potential energy. The kinetic energy terms, $\frac{1}{2}m_1\frac{\delta\bar{x_1}}{\delta t}$ and $\frac{1}{2}m_2\frac{\delta\bar{x_2}}{\delta t}$, account for the motion of each body, while $U(r)$ is the gravitational potential energy, which depends on the distance **r** between the two bodies. The total energy E_{tot} remains constant in a closed system and helps in analyzing the stability and dynamics of the orbit.

The relative acceleration equation is expressed as:

$$\frac{\delta\bar{v}}{\delta t} = \frac{\mu\bar{r}}{r^3} \quad (2)$$

Equation 2 describes the derivative of velocity v which is acceleration a, between the two bodies in the system. This derivative is derived from the rate of change of the separation distance r and indicates how quickly the velocity between the two bodies is changing due to their mutual gravitational attraction. Understanding this relative acceleration is crucial for predicting the future positions of the bodies and for calculating their orbital trajectories. The orbital position equation is given by:

$$r = \frac{h^2}{\mu(1+ecos\theta)(cos\theta\,\hat{p}+sin\theta\,\hat{q})} \tag{4}$$

Equation 4 represents the position vector r in an orbital system, where h is the specific angular momentum, e is the orbital eccentricity, and θ is the true anomaly. The terms $\hat{p}$ and $\hat{q}$ describe the coordinates in the orbital plane. This equation is fundamental for describing the elliptical orbit of the bodies, showing how the position changes with the true anomaly and eccentricity. The orbital velocity equation is expressed as:

$$\bar{v} = \frac{\mu}{h(-sin\theta+(e+cos\theta))\hat{q}} \tag{5}$$

Equation 5 provides the velocity $\bar{v}$ of the orbiting body, where h represents the specific angular momentum, θ is the true anomaly, and e is the orbital eccentricity. The terms $-\,sin\theta\,+\,(e\,+\,cos\theta)\hat{p}$ account for the components of the velocity in the orbital plane. This equation is crucial for understanding the speed of the body along its orbit and for calculating the orbital parameters and dynamics.

Frames:
The perifocal frame is a natural reference frame for analyzing Keplerian orbits, centered at the focus of the orbit and aligning with its geometric properties. Its x-axis($\hat{p}$) points from the focus through periapsis, the y-axis ($\hat{q}$) is orthogonal to $\hat{p}$ in the orbital plane, and the z-axis($\hat{w}$) is perpendicular to the orbital plane, aligned with the angular momentum vector. This formulation simplifies the kinematics of orbital motion, providing a foundation for more complex three-dimensional orbital analyses.

Keplerian elements offer a simplified, idealized approximation of an orbit, essential for predicting the motion of celestial bodies. The precise understanding of orbital elements facilitates advancements in space exploration, satellite deployment, and the study of celestial mechanics. However, real orbits experience changes due to gravitational perturbations and relativistic effects, necessitating continuous adjustment of these elements for accurate modeling. This continuous adjustment is crucial as it ensures the precision and reliability of orbital predictions, which is vital for mission success and the safe operation of satellites.

In orbital mechanics, several fundamental physics equations of motion are essential for describing and predicting the behavior of celestial bodies. These equations encompass the forces involved, the derivatives of position and velocity, and the overall dynamics of motion.

$$\bar{F} = m\bar{A} \tag{6}$$

Equation 6 is Newton's second law, which states that the force F acting on an object is equal to its mass m multiplied by its acceleration A. In the context of orbital mechanics, this law is foundational, as it describes how the gravitational forces cause celestial bodies to accelerate and change their motion.

$$F = \frac{GMm}{r^2} \tag{7}$$

Equation 7 represents the gravitational force between two masses M and m, separated by a distance r^2. Here, G is the gravitational constant (6.67*10^11). This inverse-square law is crucial for understanding the attractive force that governs the motion of planets, satellites, and other celestial bodies within their orbits.

$$F = \frac{\mu m}{r^2} \tag{8}$$

Equation 8 describes the force F acting on a mass m due to a central body with gravitational parameter μ, at a distance r. This equation is fundamental in orbital mechanics, as it simplifies the calculation of gravitational forces in a two-body system by using μ, which is specific to the central body like Earth or the Sun.

$$Derivative\ of\ position = v = \frac{\delta\bar{r}}{\delta t} \tag{9}$$

Equation 9 states that the derivative of position $\bar{r}$ with respect to time is the velocity v. It highlights the relationship between a body's position and its velocity, which is fundamental for tracking the motion of orbiting bodies over time. Knowing the velocity allows us to determine how the position of a satellite changes, providing insights into its trajectory.

$$Derivative\ of\ velocity = a = \frac{\delta\bar{v}}{\delta t} \tag{10}$$

Equation 10 expresses that the derivative of velocity $\bar{v}$ with respect to time is the acceleration a. It signifies how the velocity of a body changes over time due to forces acting on it, such as gravity. Acceleration is a key quantity in determining how the speed and direction of a satellite's motion evolve under gravitational influences.

$$\frac{\delta\bar{X}}{\delta t} = f(\bar{x})$$

(11)

Equation 11 represents the derivative of the position vector $\frac{\delta \bar{X}}{\delta t}$ with respect to time, which is the velocity **v**. In orbital mechanics, this relationship is crucial as it describes how the position of a celestial body changes over time. Knowing the velocity allows for the prediction of the body's future position along its orbital path.

$$\frac{\delta\delta \bar{X}}{\delta\delta t} = -\frac{\mu}{r^3} r$$

(12)

Equation 12 describes the acceleration $\frac{\delta\delta \bar{X}}{\delta\delta t}$ of a body under the influence of gravity in vector form. Here, X is the position vector, μ is the standard gravitational parameter, and r is the distance between the two bodies. This form of Newton's second law in a gravitational field shows how the gravitational force affects the body's motion, providing insights into the orbital dynamics.

$$\bar{x} = [\bar{r}\ \bar{v}] = [x,\ y,\ z,\ \dot{x},\ \dot{y},\ \dot{z}]$$

(13)

This vector notation, equation 13, represents the initial state vector, combining position $[x,\ y,\ z]$ and velocity $[\dot{x},\ \dot{y},\ \dot{z}]$. This state vector is used to initialize the equations of motion in numerical simulations and integrators. It serves as the starting point for predicting future states of the system.

$$\dot{\bar{x}} = [\bar{v}\ \bar{A}] = [\dot{x},\ \dot{y},\ \dot{z},\ -\frac{\mu}{r^3}x,\ -\frac{\mu}{r^3}y,\ -\frac{\mu}{r^3}z]$$

(14)

Equation 14 extends the state vector to include acceleration A, where the terms $[-\frac{\mu}{r^3}x,\ -\frac{\mu}{r^3}y,\ -\frac{\mu}{r^3}z]$ represent the accelerations due to gravitational forces.

Numerical Integration (Runge-Kutta Method)

Numerical integrators, such as the Runge-Kutta method, are used to solve differential equations in orbital mechanics. These integrators compute the future state of a system based on its current state and the rates of change. The Runge-Kutta method, in particular, provides a robust and accurate way to integrate the equations of motion over time, enabling precise predictions of orbital trajectories.

By leveraging these fundamental equations and numerical methods, orbital mechanics can accurately model and predict the complex motions of celestial bodies in space.

Third Body Perturbation

In orbital mechanics, third-body perturbations arise from the gravitational influence of celestial bodies other than the primary Earth and the orbiting satellite. For instance, consider a satellite in low Earth orbit where the primary perturbations come from Earth's oblateness and atmospheric drag. Introducing third bodies, such as the Sun and Moon, adds additional gravitational forces that can alter the satellite's orbit, causing slight changes in parameters like eccentricity and inclination. These perturbations are modeled by considering the Sun and Moon as point masses, simplifying the complex gravitational interactions. To obtain accurate positions of the Sun and Moon, NAIF SPICE kernels for a specific epoch are used, ensuring precise and reliable data for the calculations.

The equations of motion for the satellite are derived by accounting for the gravitational forces exerted by both the Earth and the third bodies (the Sun and Moon). The resulting acceleration is influenced by the gravitational pull from these celestial bodies, leading to perturbative forces that act opposite to the satellite's position vectors relative to the Sun and Moon. While these third-body perturbations introduce subtle variations in the satellite's orbit, they are typically minimal compared to the dominant effects of Earth's oblateness and atmospheric drag. However, over time, these perturbations are crucial for accurately predicting satellite orbits, as they can lead to deviations from expected paths.

The generalized form of third-body acceleration incorporates the sum of influences from multiple third bodies, emphasizing the need to account for these effects in precise orbital mechanics calculations. This highlights the nuanced but often minor influence of third-body effects in the context of more substantial perturbations, ensuring the overall shape and characteristics of the orbit remain largely unchanged, maintaining a near-consistent trajectory.

Major Equations for Third-Body Perturbations:

$$a_{third\ body} = -\mu_{sun}\left(\frac{r-r_{sun}}{\left|r-r_{sun}\right|^3} + \frac{r_{sun}}{r_{sun}^{\ 3}}\right) - \mu_{moon}\left(\frac{r-r_{moon}}{\left|r-r_{moon}\right|^3} + \frac{r_{moon}}{r_{moon}^{\ 3}}\right) \tag{15}$$

Equation 15 describes the acceleration on a satellite due to the gravitational perturbations from both the Sun and the Moon. These terms represent the differential gravitational forces exerted by these third bodies on the satellite, causing deviations in its orbit that must be considered for precise orbital predictions.

$$r_{ES} = r_S - r_E \tag{16}$$

Equation 16 represents the vector distance r_{ES} between the Earth (E) and the Sun (S). Here, r_S is the position vector of the Sun, and r_E is the position vector of the Earth. This distance is fundamental for calculating the gravitational influence of the Sun on the satellite orbiting Earth.

$$\frac{\delta\delta r_{ES}}{\delta\delta t} = \frac{\delta\delta r_S}{\delta\delta t} - \frac{\delta\delta r_E}{\delta\delta t}$$

(17)

Equation 17 gives the second time derivative of the Earth-Sun distance vector, representing the relative accelerations of the Earth and the Sun. It is crucial for understanding the dynamic changes in the distance between the Earth and the Sun, influenced by their mutual gravitational attractions and those of other celestial bodies.

$$\sum F_E = m_E \frac{\delta\delta r_E}{\delta\delta t} = \frac{G m_E m_S r_{ES}}{r_{ES}^3} + \frac{G m_E m_{EM}}{r_{EM}^3}$$

(18)

Equation 18 describes the total gravitational force acting on the Earth, considering contributions from both the Sun and the Moon. Here, m_E is the mass of the Earth, m_S is the mass of the Sun, m_M is the mass of the Moon, r_{ES} is the Earth-Sun distance vector, and r_{EM} is the Earth-Moon distance vector.

$$\frac{\delta\delta r}{\delta\delta t} = -\frac{G(m_E)r}{r^3} - G\sum_{i=1}^{n} m_i\left(\frac{r-r_i}{|r-r_i|^3} + \frac{r_i}{r_i^3}\right)$$

(19)

Equation 19 generalizes the concept of third-body perturbations to include multiple perturbing bodies. It shows the total acceleration on a satellite due to Earth's gravity and the additional gravitational influences from n other bodies (e.g., the Sun, Moon, and other planets). Each term in the summation represents the perturbative effect of one of these additional bodies.

By understanding and applying these equations, one can accurately model the complex third-body gravitational interactions that affect the orbits of satellites and other celestial objects, leading to more precise predictions of their trajectories.

In a 24-hour period, an object starting from a position 7,000 km along the x-axis, with an initial velocity of 7.72 km/s in the y-direction and 5 km/s in the z-direction, travels through space at a 90-degree angle relative to its starting point. The simulation was conducted with an initial epoch of January 1, 2020, using precise data for the positions of the Sun and Moon obtained from NAIF SPICE kernels.

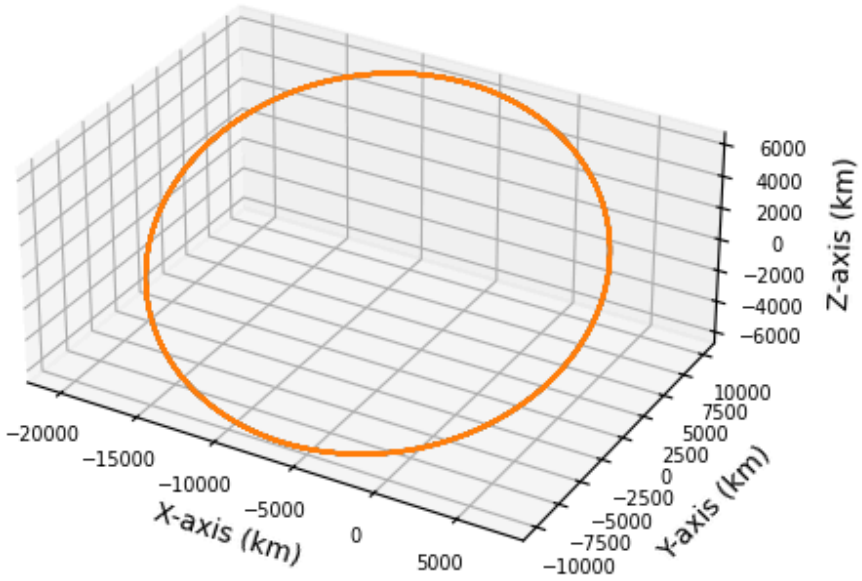

Figure 4: Orbital Plot w/ Third Body Perturbations

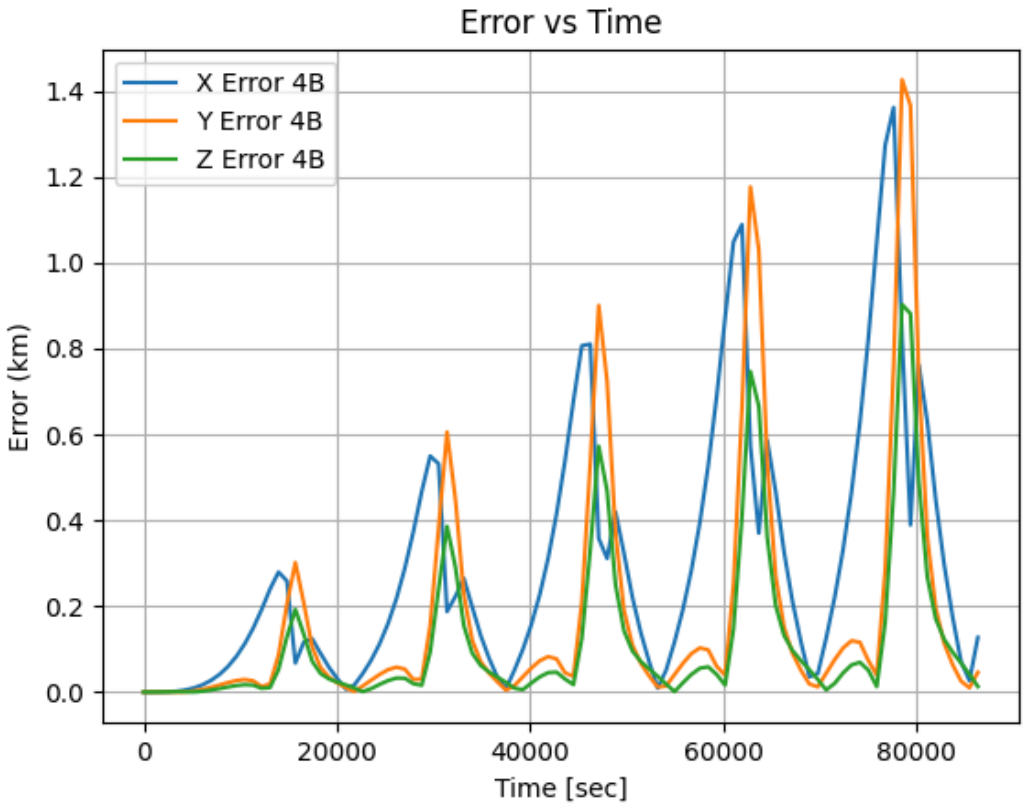

Figure 5: Error vs Time Graph of Third Body Perturbations

Figure 4 illustrates the discrepancies in the X, Y, and Z coordinates of a satellite's predicted position over time when considering four-body perturbations. The X Error, Y Error, and Z Error are plotted in blue, orange, and green, respectively. The horizontal axis represents time in seconds, ranging from 0 to approximately 86,400 seconds (or one day), while the vertical axis shows the error in kilometers, with peaks reaching up to about 1.4 km.

This plot demonstrates how the positional errors in the satellite's orbit evolve over a 24-hour period due to perturbative forces from additional celestial bodies like the Sun and Moon. The periodic nature of the errors indicates that these perturbations have a cyclical impact on the satellite's trajectory. Peaks in the graph signify times when the satellite's position deviates most significantly from its predicted path, likely corresponding to specific alignments or positions relative to the perturbing bodies. Overall, the graph underscores the importance of accounting for third-body effects in orbital mechanics to maintain accurate satellite tracking and prediction.

The bottom graph presents the positional errors in the satellite's X, Y, and Z coordinates due to third-body perturbations, particularly from the gravitational influences of the Sun and Moon, over a period of time. The error magnitudes are shown in kilometers, plotted against time in seconds, to demonstrate how these third-body forces cumulatively affect the satellite's trajectory. By comparing the base orbit with the perturbed orbit and analyzing the error trends, the figures collectively emphasize the significance of accurately accounting for third-body perturbations in orbital mechanics for precise satellite navigation and mission planning.

Earth Oblateness

Earth's oblateness refers to the phenomenon where the planet is not a perfect sphere but rather an oblate spheroid, meaning it is slightly flattened at the poles and bulging at the equator. This shape is primarily due to the Earth's rotation, which causes a centrifugal force to push the equatorial region outward. The equatorial diameter is about 43 kilometers (27 miles) greater than the polar diameter. This oblateness affects various aspects of Earth's gravitational field, influencing satellite orbits and global sea levels. Additionally, it contributes to distributing the planet's mass and the dynamics of its atmosphere and oceans.

The J2 derivation, often referred to as the second zonal harmonic, is a key parameter in the field of geodesy and astrodynamics that quantifies the extent of Earth's oblateness. It represents the deviation of Earth's gravitational field from that of a perfect sphere, focusing on the equatorial bulge. J2 is critical in predicting satellite orbits, as it causes perturbations due to the uneven distribution of mass around the planet. Calculations involving J2 allow for more accurate models of satellite trajectories, orbital decay, and the precession of orbital planes. Understanding and incorporating J2 is essential for precise navigation, Earth observation missions, and the study of gravitational interactions within the Earth-Moon system and beyond.

$$Oblateness = \frac{Equatorial\ Radius - Polar\ Radius}{Equatorial\ Radius} \quad (20)$$

Equation 20 describes how much the Earth's shape deviates from a perfect sphere. The difference between the equatorial and polar radii, divided by the equatorial radius, gives a measure of the Earth's flattening at the poles. This oblateness must be considered in orbital mechanics because it affects the gravitational potential experienced by satellites, especially those in low Earth orbit. The bulging at the equator, caused by the Earth's rotation, introduces additional forces that perturb satellite orbits, necessitating adjustments to predictions and models to ensure accuracy.

$$u_{J_2} = \frac{\mu J_2 R_\oplus^{\ 2}}{2r^3}(1 - 3\,sin^2 \varnothing) \tag{21}$$

Equation 21 represents the perturbative potential u_{J_2} due to Earth's oblateness (J2 effect). The values and constants in this context are critical for understanding the perturbative forces acting on a satellite in orbit around Earth. The gravitational parameter of Earth (μ), given as 398600.441500 km^3/s^2, represents the product of the gravitational constant and the mass of Earth, crucial for calculating gravitational forces. The coefficient J_2, valued at 0.00108264, quantifies the Earth's oblateness, indicating how much the Earth's shape deviates from a perfect sphere due to its equatorial bulge. The Earth's mean radius $R_\oplus$, set at 6378.00 km, is essential for scaling the oblateness effect and calculating the gravitational potential at a given distance from the Earth's center. The equation also incorporates the factor $(1 - 3\,sin^2 \varnothing)$, which accounts for the variation of the potential with latitude, where $\varnothing$ represents the satellite's latitude. This perturbative potential is critical for precise orbital mechanics calculations, especially for low Earth orbits where the J2 effect significantly influences orbital elements such as precession and inclination.

The gravitational potential u in a spherical harmonic expansion can be expressed as:

$$u = \frac{\mu}{r}\sum_{n=0}^{\infty}\sum_{m=0}^{n}\left(\frac{R_\oplus}{r}\right)^n P_{n_1 m}(sin\ \varnothing)[c_{n_1 m}cos(m\lambda) + s_{n_1 m}sin(m\lambda)] \tag{22}$$

Equation 22 describes the gravitational potential u using a series expansion in terms of spherical harmonics. Here, $R_\oplus$ is the Earth's mean radius, r is the radial distance from the Earth's center, $P_{n_1 m}$ is the associated Legendre polynomials, Θ is the colatitude, and λ is the longitude. The coefficients $c_{n_1 m}$ and $s_{n_1 m}$ represent the gravitational potential coefficients for cosine and sine terms, respectively. This expansion allows for the precise modeling of the Earth's gravitational field by considering higher-order terms that account for irregularities in the Earth's shape, providing a more accurate representation of the forces acting on a satellite.

The gravitational acceleration a_g^{ECEF} in Earth-Centered Earth-Fixed (ECEF) coordinates is given by:

$$a_g^{ECEF}(r^{ECEF}, \Theta) = -\frac{\mu}{r^2}u^{ECEF} + \sum_{l=2}^{\infty}\frac{\mu J_l}{r^2}\left(\frac{R_E}{r}\right)^l u_{J_l} \tag{23}$$

Equation 23 describes the total gravitational acceleration experienced by a satellite in ECEF coordinates. The term $\frac{\mu}{r^2}u^{ECEF}$ represents the primary gravitational acceleration, where μ is the gravitational parameter of Earth and r is the distance from the Earth's center. The summation term accounts for the perturbative effects due to the Earth's oblateness (J2 effect). The factor $\left(\frac{R_E}{r}\right)^l u_{J_l}$ scales the perturbative potential with the satellite's distance, providing a detailed description of the gravitational forces in ECEF coordinates. This comprehensive equation is crucial for accurate modeling and prediction of satellite orbits, ensuring that all significant gravitational perturbations are considered.

In a 24-hour period, an object starting from a position 7,000 km along the x-axis, with an initial velocity of 7.72 km/s in the y-direction and 5 km/s in the z-direction, with a displacement that forms a 90-degree theta relative to its starting point.

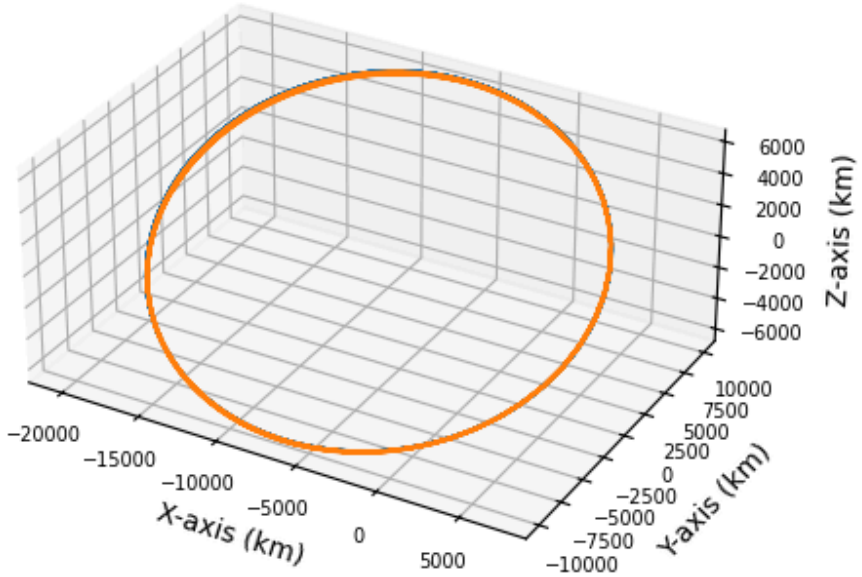

Figure 6: Orbital Plot w/ J2 Perturbations

In this orbital plot, the J2 perturbation—resulting from Earth's oblateness—exerts a significant yet often subtle influence on the satellite's trajectory. While the effects of J2 might not be immediately visible in short-term observations, they are substantial over longer periods. The

perturbation causes gradual, periodic shifts in the satellite's orbit, affecting parameters such as inclination and the orientation of the orbit. Although these changes might be minor on a daily or weekly basis and may not show dramatic deviations from the initial path, they accumulate over time, leading to significant long-term variations. This subtle yet impactful effect requires careful monitoring and analysis to ensure precise orbital predictions and adjustments, underscoring its importance in mission planning and satellite operations.

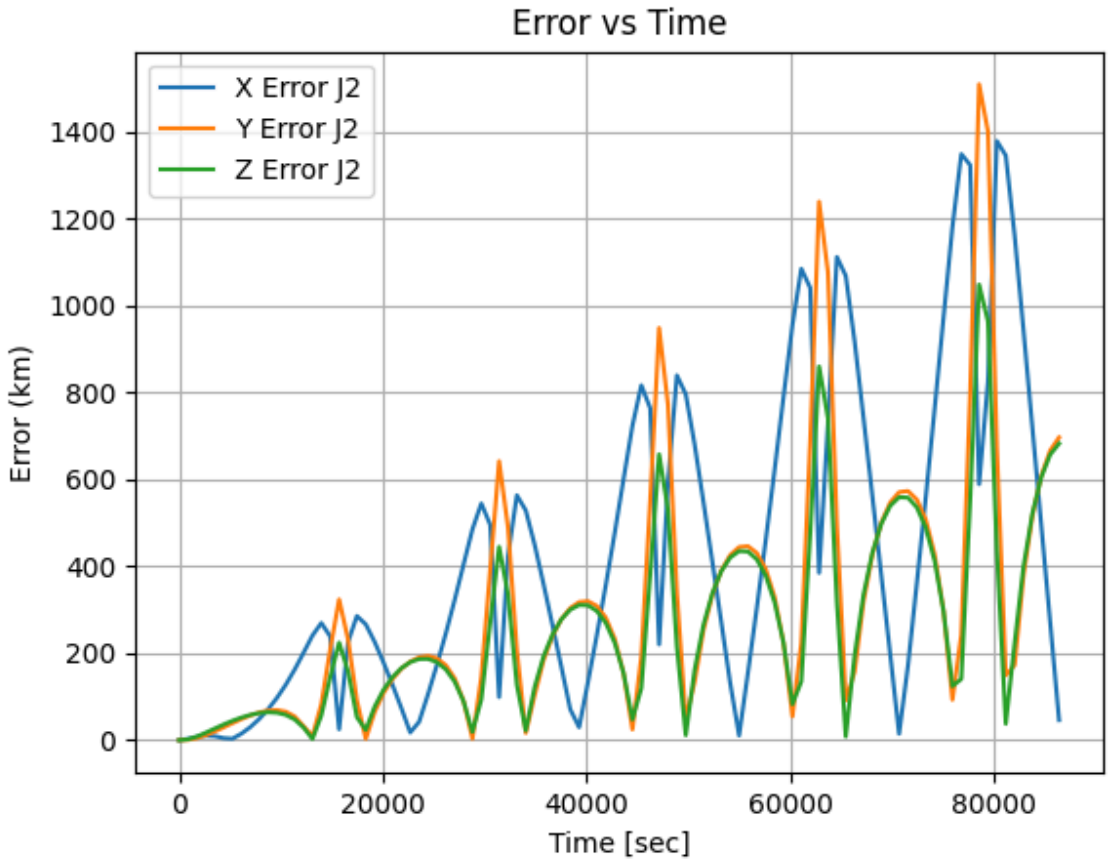

Figure 7: Error vs Time Graph of J2 Perturbations

The provided graph illustrates the positional errors in the X, Y, and Z dimensions of a satellite's orbit over time due to the Earth's oblateness (J2 effect). The errors exhibit a periodic pattern, with the X and Y errors showing significant fluctuations, peaking above 1400 km, while the Z error remains comparatively lower. This periodic increase in error indicates the regular perturbations in the satellite's orbit caused by the equatorial bulge of the Earth, which leads to deviations from the expected trajectory. Understanding and accurately modeling these perturbations are crucial for maintaining precise satellite operations, as uncorrected errors can significantly impact navigation, mission planning, and collision avoidance in low Earth orbits.

Atmospheric Drag

Atmospheric drag is a significant perturbation force acting on satellites in low Earth orbit (LEO), particularly as they pass through the thermosphere at altitudes above 200 km. This drag force leads to the exchange of energy and momentum between the satellite and the atmosphere, causing a gradual decay in the satellite's orbit. Accurate modeling of atmospheric drag is crucial for predicting satellite trajectories, ensuring precise orbit determination, aiding in collision avoidance, and planning for re-entry predictions. Uncertainties in thermospheric mass density (TMD) contribute to the difficulty in predicting atmospheric drag, impacting the overall accuracy of orbit predictions.

Atmospheric drag is caused by the interaction between a satellite and the Earth's atmosphere. As a satellite travels through the upper layers of the atmosphere, it encounters atmospheric particles, despite the low density at these altitudes. The satellite's relative velocity to these particles results in a transfer of linear momentum, leading to a deceleration force opposite to its direction of motion. Factors such as the density of atmospheric particles, satellite surface area, and the velocity of the satellite relative to the Earth's rotating atmosphere contribute to the magnitude of this drag force.

Atmospheric drag is modeled by considering the density of atmospheric particles at the satellite's altitude, the satellite's surface area, and its velocity relative to the atmosphere. The basic drag acceleration formula incorporates these parameters, along with a drag coefficient C which varies based on the satellite's shape and surface properties. The relative velocity is computed by considering the satellite's motion in an Earth-centered inertial (ECI) frame and accounting for the Earth's rotation and atmospheric winds. Advanced models also integrate empirical and physical TMD models, such as the MSIS, Jacchia, and DTM models, to provide more accurate representations of atmospheric density and variability. These models help refine the predictions of drag forces and their effects on satellite orbits over time. The equation of motion for the drag acceleration a_{drag} on a satellite is given by:

$$a_{drag} = -\frac{C}{2}\rho(r)\frac{A}{m}v'^{2}\frac{v'}{|v'|} \tag{24}$$

Equation 24 describes the deceleration experienced by a satellite due to atmospheric drag. Here, C is the drag coefficient, a dimensionless number representing the satellite's shape and surface characteristics affecting drag. The term $\rho(r)$ is the atmospheric density at the satellite's altitude r, which varies with altitude. The ratio $\frac{A}{m}$ represents the satellite's cross-sectional area A to its mass m, indicating how much drag force is applied per unit mass. The term v' is the satellite's velocity relative to the atmosphere, and $v'^{2}\frac{v'}{|v'|}$ combines the square of the relative velocity (magnitude) with the unit vector of the velocity direction, ensuring the drag force opposes the satellite's motion. This equation is crucial for modeling the orbital decay of low Earth orbit satellites, as atmospheric drag significantly impacts their trajectories, causing a gradual reduction in altitude and eventual re-entry into the Earth's atmosphere.

Earth Satellite Parameters

	25	26	27	28	29	30	31	32
		ATMOSPHERIC DENSITY			ΔV TO MAINTAIN ALTITUDE			
Alt (km)	Atm. Scale Ht. (km)	Minimum (kg/m^3)	Mean (kg/m^3)	Maximum (kg/m^3)	Solar Min 50 kg/ m^2 (m/s)/yr	Solar Max 50 kg/ m^2 (m/s)/yr	Solar Min 200 kg/ m^2 (m/s)/yr	Solar Max 200 kg/ m^2 (m/s)/yr
0	8.4	1.2	1.2	1.2	2.37×10^{13}	2.37×10^{13}	5.92×10^{12}	5.92×10^{12}
100	5.9	4.61×10^{-7}	4.79×10^{-7}	5.10×10^{-7}	8.95×10^{8}	9.90×10^{8}	2.24×10^{8}	2.47×10^{8}
150	25.5	1.65×10^{-9}	1.81×10^{-9}	2.04×10^{-9}	3.17×10^{4}	3.94×10^{4}	7.93×10^{3}	9.85×10^{3}
200	37.5	1.78×10^{-10}	2.53×10^{-10}	3.52×10^{-10}	3.40×10^{3}	6.72×10^{3}	8.51×10^{2}	1.68×10^{3}
250	44.8	3.35×10^{-11}	6.24×10^{-11}	1.06×10^{-10}	6.36×10^{2}	2.02×10^{3}	1.59×10^{2}	5.04×10^{2}
300	50.3	8.19×10^{-12}	1.95×10^{-11}	3.96×10^{-11}	1.54×10^{2}	7.47×10^{2}	3.86×10^{1}	1.87×10^{2}
350	54.8	2.34×10^{-12}	6.98×10^{-12}	1.66×10^{-11}	4.37×10^{1}	3.11×10^{2}	1.09×10^{1}	7.78×10^{1}
400	58.2	7.32×10^{-13}	2.72×10^{-12}	7.55×10^{-12}	1.36×10^{1}	1.40×10^{2}	3.40×10^{0}	3.50×10^{1}
450	61.3	2.47×10^{-13}	1.13×10^{-12}	3.61×10^{-12}	4.55×10^{0}	6.66×10^{1}	1.14×10^{0}	1.66×10^{1}
500	64.5	8.98×10^{-14}	4.89×10^{-13}	1.80×10^{-12}	1.64×10^{0}	3.29×10^{1}	4.11×10^{-1}	8.23×10^{0}
550	68.7	3.63×10^{-14}	2.21×10^{-13}	9.25×10^{-13}	6.59×10^{-1}	1.68×10^{1}	1.65×10^{-1}	4.20×10^{0}
600	74.8	1.68×10^{-14}	1.04×10^{-13}	4.89×10^{-13}	3.03×10^{-1}	8.81×10^{0}	7.58×10^{-2}	2.20×10^{0}
650	84.4	9.14×10^{-15}	5.15×10^{-14}	2.64×10^{-13}	1.64×10^{-1}	4.73×10^{0}	4.09×10^{-2}	1.18×10^{0}
700	99.3	5.74×10^{-15}	2.72×10^{-14}	1.47×10^{-13}	1.02×10^{-1}	2.61×10^{0}	2.55×10^{-2}	6.52×10^{-1}
750	121	3.99×10^{-15}	1.55×10^{-14}	8.37×10^{-14}	7.04×10^{-2}	1.48×10^{0}	1.76×10^{-2}	3.69×10^{-1}
800	151	2.96×10^{-15}	9.63×10^{-15}	4.39×10^{-14}	5.19×10^{-2}	8.63×10^{-1}	1.30×10^{-2}	2.16×10^{-1}
850	188	2.28×10^{-15}	6.47×10^{-15}	3.00×10^{-14}	3.97×10^{-2}	5.23×10^{-1}	9.94×10^{-3}	1.31×10^{-1}
900	226	1.80×10^{-15}	4.66×10^{-15}	1.91×10^{-14}	3.11×10^{-2}	3.30×10^{-1}	7.78×10^{-3}	8.25×10^{-2}
950	263	1.44×10^{-15}	3.54×10^{-15}	1.27×10^{-14}	2.48×10^{-2}	2.18×10^{-1}	6.19×10^{-3}	5.45×10^{-2}
1,000	296	1.17×10^{-15}	2.79×10^{-15}	8.84×10^{-15}	1.99×10^{-2}	1.51×10^{-1}	4.98×10^{-3}	3.77×10^{-2}
1,250	408	4.67×10^{-16}	1.11×10^{-15}	2.59×10^{-15}	7.69×10^{-3}	4.27×10^{-2}	1.92×10^{-3}	1.07×10^{-2}
1,500	516	2.30×10^{-16}	5.21×10^{-16}	1.22×10^{-15}	3.68×10^{-3}	1.95×10^{-2}	9.20×10^{-4}	4.88×10^{-3}
2,000	829	—	—	—	—	—	—	—
2,500	1,220	—	—	—	—	—	—	—
3,000	1,590	—	—	—	—	—	—	—

Graph from *Space Traffic Management* by Carolin Frueh

Figure 6: Atmospheric Density with Scale Heights

The table illustrates how atmospheric density decreases significantly with altitude, affecting the drag on satellites. The ΔV values indicate how much propulsion effort is needed to counteract this drag and maintain a stable orbit, with variations due to solar activity and the satellite's area-to-mass ratio. During solar maximum, increased solar activity heats and expands the Earth's atmosphere, increasing atmospheric drag on satellites, which requires greater ΔV to

maintain their orbits. Conversely, during solar minimum, the atmosphere contracts, reducing drag and thus the required ΔV. This table is essential for satellite mission planning and operations, providing necessary data to ensure long-term orbital stability and proper functioning of Earth-orbiting satellites.

In a 24-hour period, an object starting from a position 7,000 km along the x-axis, with an initial velocity of 7.72 km/s in the y-direction and 5 km/s in the z-direction. The major assumptions made here include selecting a C value of 2, assuming an altitude of 100 km with a corresponding atmospheric density $\rho(r)$=0.0000000461 kg/m^3, considering a spherical cross-sectional area of $10^{-3}m^2$, and a mass of 5 kg for the object.

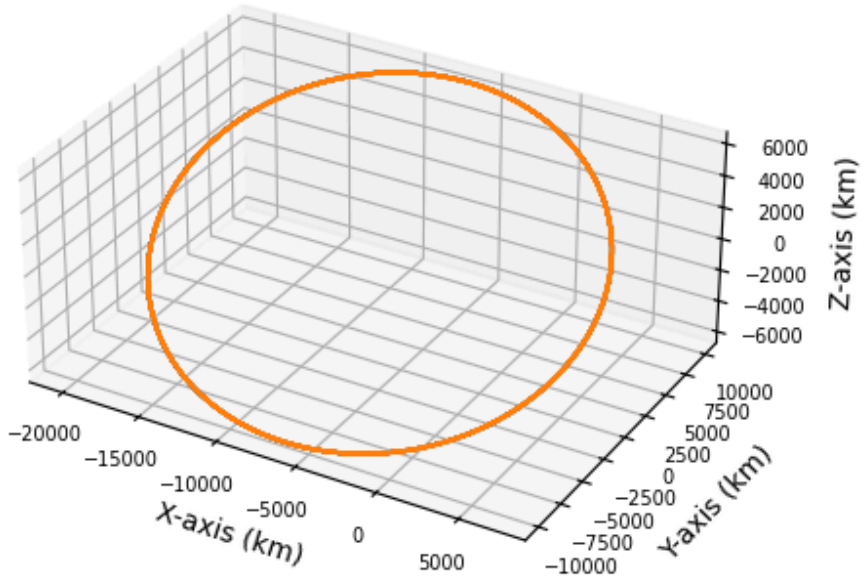

Figure 8: Orbital Plot w/ Drag Perturbations

In an orbital plot affected by atmospheric drag, the trajectory of a satellite in low Earth orbit shows subtle yet significant alterations compared to its initial path. Atmospheric drag, being the second-largest perturbation after J2 (Earth's oblateness), exerts a continuous decelerating force on the satellite. This force gradually lowers the satellite's altitude and modifies its orbital shape over time. On an orbital plot, these changes might not be immediately evident due to their gradual nature. The satellite's orbit might appear nearly identical to the original path on a short-term scale, but over extended periods, the plot reveals a noticeable trend of decreasing altitude and increased orbital decay. While the effects are more pronounced than third-body perturbations, they are less dramatic than those caused by J2, requiring careful analysis to understand their full impact on the satellite's long-term trajectory and mission planning.

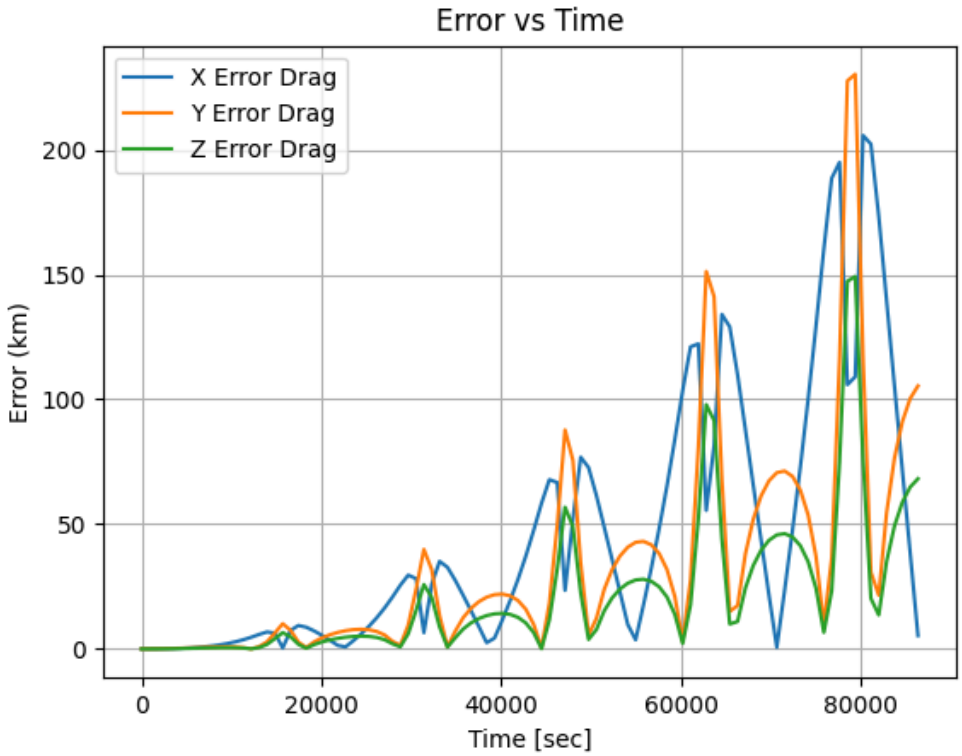

Figure 9: Orbital Plot w/ Third Body Perturbations

The graph illustrates the positional errors in the X, Y, and Z dimensions of a satellite's orbit over time due to atmospheric drag, showing a periodic pattern with generally lower magnitudes compared to the J2 effect. The X Error Drag (blue line) displays the most significant variations, peaking above 200 km, followed by the Y Error Drag (orange line), while the Z Error Drag (green line) is the smallest. The periodic peaks indicate the influence of orbital characteristics and the satellite's interaction with varying atmospheric density. These errors underscore the importance of accounting for atmospheric drag in orbital mechanics to predict orbital decay and ensure precise satellite navigation, necessitating adjustments to maintain the desired orbit and optimize satellite operations.

Discussion

In the study of orbital mechanics, understanding the various forces and perturbations that influence the trajectories of satellites is crucial for precise modeling and prediction. The primary two-body problem, which simplifies the dynamics of interactions between a satellite and a central body like Earth, serves as a foundational framework. However, real-world orbital calculations require a more nuanced approach that incorporates additional perturbative forces. These perturbations arise from a variety of sources, including the non-uniform distribution of Earth's mass, interactions with the Earth's atmosphere, and gravitational influences from other celestial bodies such as the Moon and the Sun. Each of these factors plays a role in altering the

orbit of a satellite, affecting its position, velocity, and trajectory over time. As these perturbations accumulate, they can lead to significant deviations from the predicted orbital path, impacting satellite operations and mission outcomes. Accurately modeling these influences is essential for a range of applications, from maintaining the precise alignment of satellite constellations to supporting scientific research and ensuring the reliability of global positioning systems. In this context, it is important to explore the various perturbative effects in detail, understanding their individual contributions and the ways they can be incorporated into predictive models to enhance accuracy and reliability in orbital mechanics.

The following figures illustrate the impact of various perturbative forces on a satellite's orbit over time. The top two images provide a three-dimensional view of the satellite's base orbit (left) and the orbit including all perturbative effects (right), highlighting the deviations introduced by these perturbations. The bottom graph presents the positional errors in the satellite's X, Y, and Z coordinates due to different perturbative effects, including atmospheric drag, Earth's oblateness (J2 effect), and additional forces, over a period of time. The error magnitudes are shown in kilometers, plotted against time in seconds, to demonstrate how these forces affect the satellite's trajectory cumulatively. By comparing the base orbit with the perturbed orbit and analyzing the error trends, the figures collectively emphasize the significance of accurately accounting for these perturbations in orbital mechanics for precise satellite navigation and mission planning.

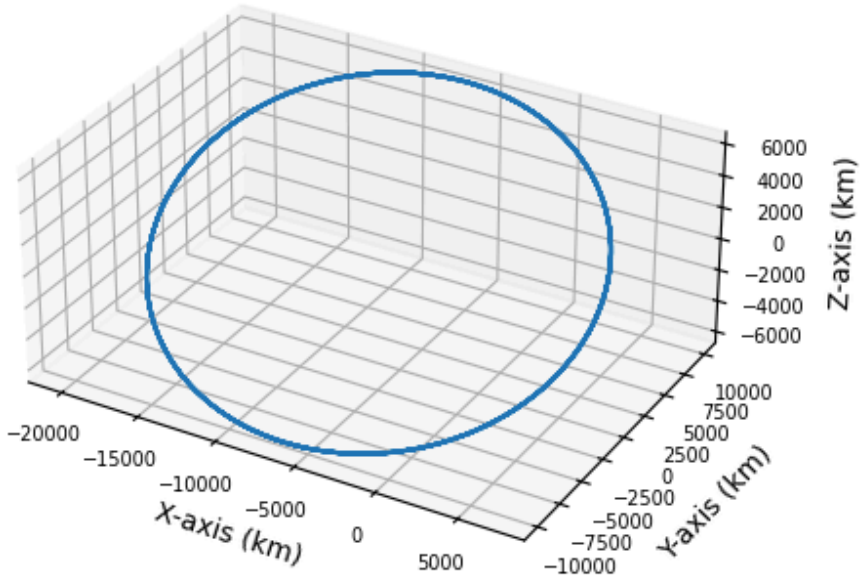

Figure 10: Orbital Plot w/ No Perturbations (Base Orbit)

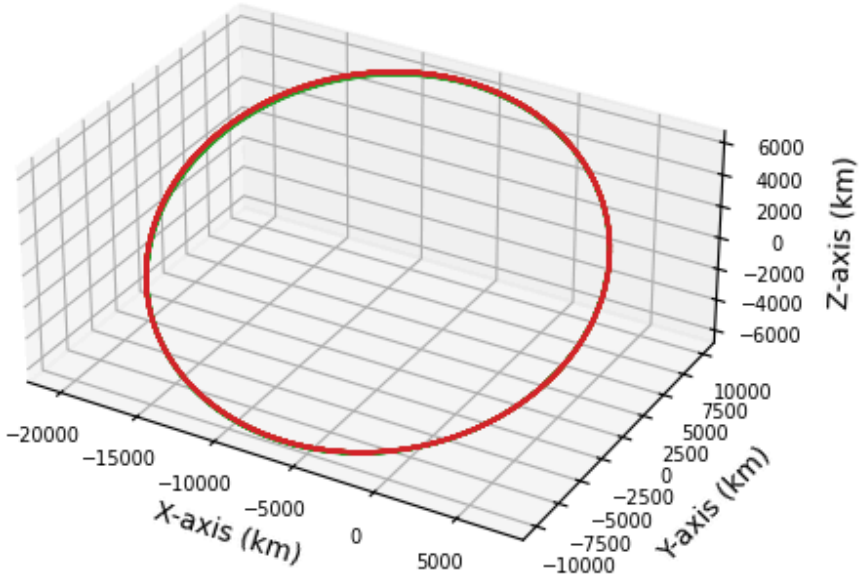

Figure 11: Orbital Plot w/ All Perturbations

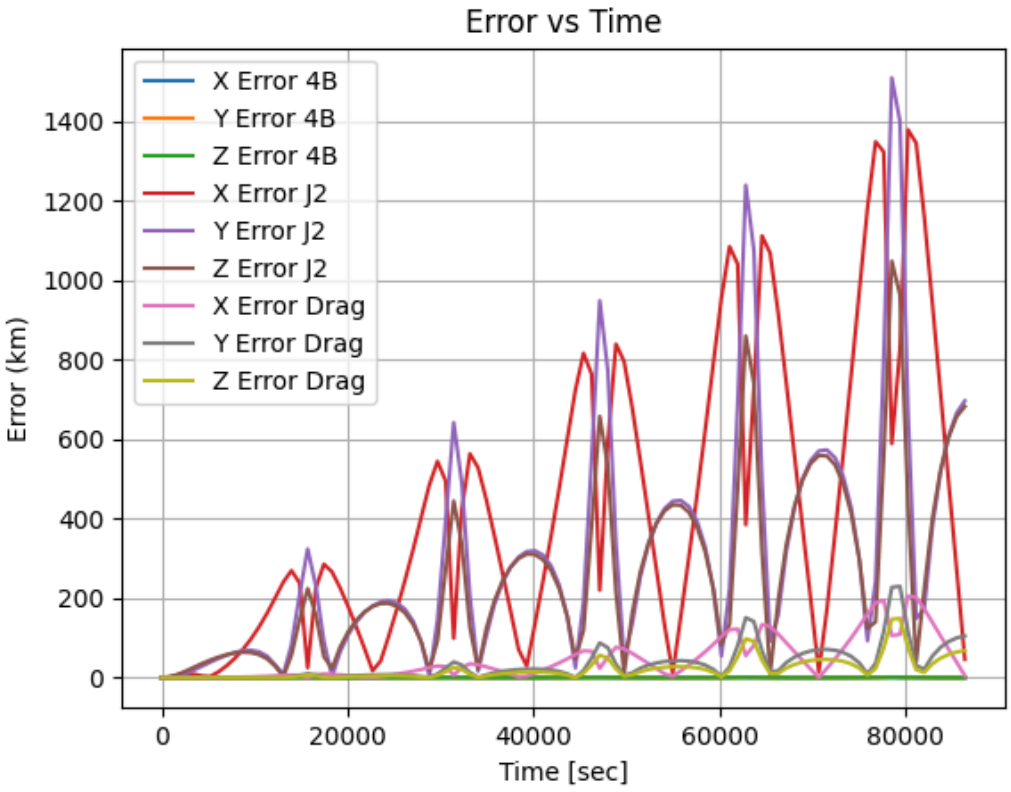

Figure 12: Error vs Time Plot of All Perturbations

Perturbation	Acceleration	Orbit Error after one Day		
		Radial	Along Track	Out of Plane
	[m/s^2]	[m]	[m]	[m]
$\frac{1}{r^2}$-Term	8.42	"∞"	"∞"	"∞"
Oblateness	$1.5 \cdot 10^{-2}$	60000	400000	900000
Atmospheric Drag	$7.9 \cdot 10^{-7}$	150	8900	1.5
Higher Terms of the Earth's Grav. Field	$2.5 \cdot 10^{-4}$	550	3400	820
Lunar Attraction	$5.4 \cdot 10^{-6}$	2	45	2
Solar Attraction	$5.0 \cdot 10^{-7}$	1	38	15
Direct Rad. Pressure	$9.7 \cdot 10^{-8}$	10	24	0
Solid Earth Tides	$1.1 \cdot 10^{-7}$	0.2	13	1
y-bias	$1.0 \cdot 10^{-9}$	0.1	4.7	0.0

Graph from *Methods of Celestial Mechanics* by *G. Beulter*

Figure 13: Accelerations acting upon LEOs (Low-Earth Orbits)

The comparison chart above, provided by *Methods of Celestial Mechanics* by G. Beutler, labels the most significant perturbation on Low Earth Orbits as Earth oblateness. Earth oblateness is followed by atmospheric drag, the R^2 term, lunar attraction, solar attraction, etc. Looking from afar via comparison plots and seeing the significance in numbers, it seems that these perturbations have a small impact on orbits over time. Although these perturbations don't provide a vast impact, it is still important when modeling/measuring precise calculations in orbital mechanics. To improve the results, it would be necessary to take into account direct solar radiation pressure and other perturbations to perfectly predict orbits. In the chart above, Earth's oblateness (the J2 effect) has the most significant impact, causing gradual precession of the orbit and affecting key orbital elements. Atmospheric drag, the second most significant perturbation, leads to altitude decay due to friction with atmospheric particles, particularly affecting low Earth orbits (LEO). Gravitational forces from the Moon and the Sun also influence satellite orbits, causing long-term changes in the semi-major axis, eccentricity, and inclination, although their effects are less pronounced than those of Earth's oblateness and atmospheric drag. Despite the seeming minor individual impacts, these perturbations accumulate over time, resulting in significant deviations from intended orbits, which is crucial for precise applications like GPS and scientific missions. Improving orbit prediction accuracy requires accounting for additional forces, such as direct solar radiation pressure, using sophisticated atmospheric density models, and integrating real-time data. By incorporating higher-order gravitational models and considering relativistic effects, predictions can be further refined. Continuously enhancing models to include a wider range of perturbative effects will enable more precise and reliable satellite trajectory predictions.

Conclusion

The work conducted on modeling the long-term stability of artificial satellites in non-equatorial orbits is crucial for ensuring the success and longevity of space missions. By understanding and quantifying the effects of various perturbations, such as Earth's oblateness, atmospheric drag, and lunar and solar gravitational forces, deviations from intended orbits can be predicted and mitigated. Results showed that Earth's oblateness had the most significant impact, causing orbital precession, while atmospheric drag led to altitude decay, particularly for low Earth orbits. Lunar and solar perturbations, although less pronounced, also contributed to long-term changes in the satellite's trajectory. Additionally, the data and conclusions from the study align with a chart from *Methods of Celestial Mechanics* by G. Beutler, further verifying the results. These findings underscore the importance of incorporating a wide range of perturbative effects in orbital mechanics models. The insights gained from this project highlight the necessity of using advanced models and real-time data to refine predictions and ensure satellites' precise and stable operation. By continuously improving the understanding and modeling of these perturbations, the reliability and effectiveness of satellite missions, which are integral to space exploration, communication, navigation, and Earth observation, are enhanced.